




Whole-body SAR measurements of millimeter-wave base station in reverberation chambers

Jens Eilers Bischoff , Paramananda Joshi, Davide Colombi, Bo Xu and Christer Törnevik

Ericsson Research, Ericsson AB, Stockholm, Sweden

Research Paper

Cite this article: Eilers Bischoff J, Joshi P, Colombi D, Xu B, Törnevik C (2024) Whole-body SAR measurements of millimeter-wave base station in reverberation chambers. *International Journal of Microwave and Wireless Technologies*, 1–6. <https://doi.org/10.1017/S1759078724000515>

Received: 14 August 2023
Revised: 9 April 2024
Accepted: 11 April 2024

Keywords:

5G; antenna measurement; reverberation chamber; wideband; whole body specific absorption rate

Corresponding author: Jens Eilers Bischoff;
Email: jens.eilers.bischoff@ericsson.com

Abstract

This paper presents a method for measuring whole-body specific absorption rate (WBSAR) of millimeter-wave base stations (BSs) in a reverberation chamber (RC). The absorbed power in the phantom from the equipment under test (EUT) and hence WBSAR is determined as the difference between the total radiated power with and without the phantom. A chamber transfer function is determined and used to include only the absorption in the phantom due to direct illumination from the EUT, i.e., excluding absorption due to the RC multipath reflections. The measurement method was evaluated at 28 GHz using a horn antenna and a commercial massive multi-input–multi-output BS. The experimental results are in good agreement with simulations. The proposed method allows for measurements of WBSAR within 3 minutes, which is much shorter than traditional approaches. The method is suitable for compliance assessments of BS products with the International Commission on Non-Ionizing Radiation Protection 2020 electromagnetic field exposure guidelines, which extend the applicability of WBSAR as basic restrictions up to 300 GHz.

Introduction

A reverberation chamber (RC) is an electrically large room with metallic walls. When the equipment under test (EUT) is transmitting in the RC, statistically uniform field strength distributions can be created through stirring. The uniform field strength distribution is equivalent to an environment of statistically uniform multipath illumination where each point is equally likely to be illuminated from all directions [1, 2]. RCs are extensively used for wireless equipment measurements, e.g., to measure the total radiated power (TRP) from wireless devices [3]. RCs are also used as exposure systems for in vivo bioassays due to their ability to generate uniform fields [2]. Dosimetric whole-body specific absorption rate (WBSAR) measurements with uniform illumination from all directions (multipath) have been performed in RCs at 1, 1.5, and 2 GHz [4]. However, the multipath propagation environment that characterizes the RC might seem, at a first glance, unsuitable to evaluate WBSAR for electromagnetic field (EMF) product compliance of a base station (BS), which is usually evaluated in free space conditions. At frequencies below 6 GHz, Kvarnstrand et al. [5] and Gifuni et al. [6] proposed a solution to isolate the contribution to the absorbed power in a phantom caused by direct illumination from a mobile phone from the power absorbed in the phantom due to the multipath illumination in the RC. In paper [7], a similar method was initially developed to assess WBSAR for BSs at millimeter-wave (mmWave) frequencies. In this paper, the method proposed in paper [7] is employed to study the exposure from an mmWave BS. Moreover, an important scenario for mmWave BS, namely beam steering, is considered in this paper. That is, for the first time, the WBSAR is evaluated, both experimentally and numerically, for different beam steering states. A part of this work was presented at the Swedish Microwave Days 2023.

Background

EMF compliance assessments of BS

When placed on the market, BS products must comply with regulatory requirements and applicable limits on human exposure to radio frequency EMFs, such as those specified by the International Commission on Non-Ionizing Radiation Protection (ICNIRP) [8]. In the ICNIRP 2020 guidelines [8], two sets of EMF exposure limits are provided, the so-called basic restrictions and reference levels. The basic restrictions relate to physical quantities in the body,

e.g., the specific absorption rate (SAR), which is defined as follows:

$$\text{SAR} = \frac{d}{dt} \left(\frac{dW}{dm} \right) \quad (1)$$

where t [s] is time, W [J] is the energy absorbed in the tissue, and m [kg] is the mass of tissue [8]. SAR can also be expressed equivalently as follows:

$$\text{SAR} = \frac{\sigma}{\rho} |E|^2 \quad (2)$$

where σ [S/m] is the conductivity of tissue, ρ [kg/m³] is the density of tissue, and E [V/m] is the root-mean-square of the induced electric field (E-field) [8]. For local exposure assessments, SAR is intended to be averaged over a cubical mass of 10 g tissue. For whole-body exposure assessment, SAR can be calculated as the total power absorbed in the body P_{abs} [W] averaged over the body mass m_{wb} [kg] [8]:

$$\text{WBSAR} = \frac{P_{abs}}{m_{wb}} \quad (3)$$

WBSAR is intended to be averaged over 30 minutes. The 2020 ICNIRP [8] guidelines extended the applicability of WBSAR up to 300 GHz compared with the previous version of the guidelines [9], while the usage of local SAR is limited to 6 GHz [8]. Reference levels, on the other hand, are defined in terms of external physical quantities, e.g., incident power density [W/m²] [8], and the limits are derived from the basic restrictions to provide a more-practical means of demonstrating compliance [8]. While compliance of mmWave BSs can be assessed by means of the reference levels [10], the availability of an efficient and accurate WBSAR measurement method is complementary to assess compliance directly with the whole-body basic restrictions introduced by ICNIRP.

Generally, the product compliance evaluation process consists of determining the BS compliance boundaries (exclusion zones) outside of which exposure is below the EMF limits (reference levels or basic restrictions). BSs are subsequently installed to prevent access to the compliance boundary. The EMF product compliance assessment of a BS is done in free space (excluding any possible impact from ambient sources and scatterers that need to be considered in an installation assessment) except for the human phantom when the evaluation is based on basic restrictions [11]. The phantoms' characteristics as well as the evaluation methods are specified in international standards, such as IEC 62232 [11]. IEC 62232 provides WBSAR measurement methods, which are generally based on scanning of the phantom with an E-field probe, applicable below 6 GHz. The same method is not directly applicable at mmWave frequencies due to the shallow field penetration depth in the phantom (of few millimeters or less) that poses substantial challenges on sensitivity and dimension of the probe. Furthermore, E-field scanning with a sub-wavelength step size requires hundreds of points to be measured, making the measurement times untenable at mmWave frequencies [11].

Measuring the TRP in an RC

To perform a TRP measurement of a EUT, the RC must be well stirred, and the RC should contain a reference antenna with known radiation efficiency and a receiving antenna. The first step is to

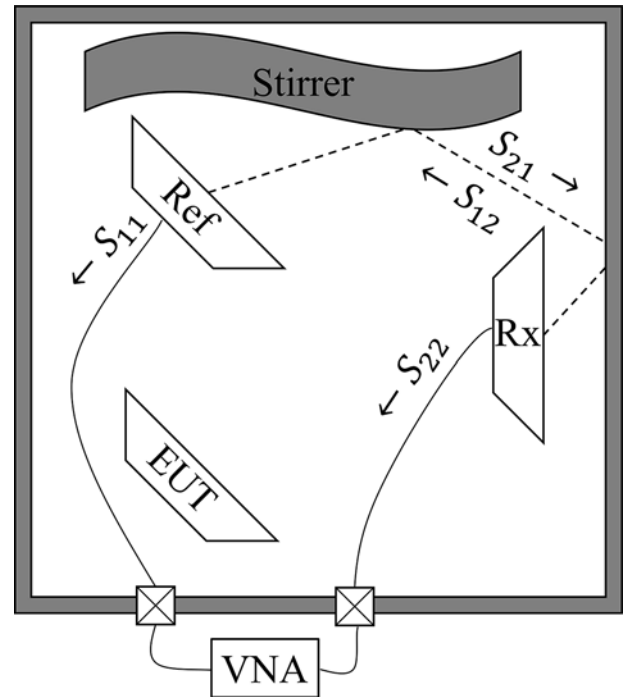


Figure 1. Illustration of the chamber transfer function measurements and the S parameters.

determine the chamber transfer function G , which is defined as [3] follows:

$$G = \frac{P_{Rx}}{P_{Tx}} \quad (4)$$

where P_{Rx} is the power received by the receiving antenna, P_{Tx} is the TRP of a source (the reference antenna or the EUT), and $\langle \rangle$ is the mean value over time. A vector network analyzer (VNA), with Port 1 connected to the reference antenna and Port 2 connected to the receiving antenna, as illustrated in Fig. 1, is used to determine G using the following equation [3]:

$$G = \frac{|S_{21}|^2}{(1 - |S_{11}|^2) \eta_{ref}} \quad (5)$$

where S_{21} is the transmission coefficient between the reference and receiving antennas, S_{11} is the reflection coefficient of the reference antenna, and η_{ref} is the known radiation efficiency of the reference antenna. Thus, $|S_{21}|^2$ is the average net power transmission from the receiving antenna to the reference antenna, and $(1 - |S_{11}|^2)$ accounts for the power loss due to reflections in the reference antenna. In a well-stirred chamber, G is independent of the source and antenna position (as long as the separation distance from the antenna to the chamber walls is larger than the reactive near-field distance [1]). As such, G is the normalized average net power transmission from any EUT to the receiving antenna [3]. Using G the TRP of a EUT is then calculated as follows [3]:

$$P_{Tx} = \frac{P_r}{GL} \quad (6)$$

where $P_r = L \cdot P_{Rx}$ is the received power measured by a spectrum analyzer and L is the losses in the cable from the receiving antenna to signal analyzer not accounted for in G in accordance with the S parameters definition in Fig. 1.

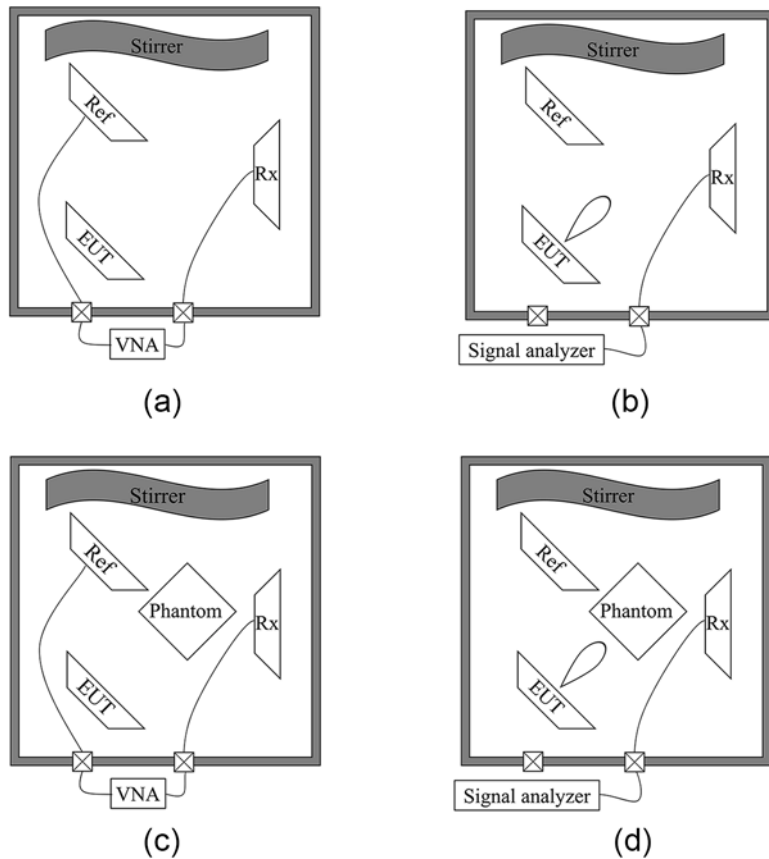


Figure 2. Diagrams of the four steps to measure WBSAR in an RC. (a) Measurement of the unloaded chamber transfer function. (b) Measurement of the EUT TRP. (c) Measurement of the loaded chamber transfer function, with the reference antenna facing away from the phantom. (d) Measurement of the net EUT TRP when the EUT is directly illuminating the phantom.

Method

Measuring WBSAR using TRP measurements

The method of measuring the TRP was extended to measure WBSAR. The chamber transfer function G_u without the phantom, i.e., the unloaded RC, was measured with a VNA and applying Equation (5), as can be seen in Fig. 2a. The received power for the EUT transmitting in the unloaded RC $P_{r|u}$ was measured with a signal analyzer (Fig. 2b), and the TRP of the EUT $P_{Tx|u}$ was calculated using Equation (6) and G_u . The phantom was then placed in the RC directly in front of the EUT and the chamber transfer function for the loaded RC, G_l , was measured with a VNA using the reference antenna and Equation (5) (Fig. 2c). The reference antenna was positioned to avoid direct illumination on the phantom, so G_l only accounted for the multipath losses including power absorbed in the phantom due to multipath illumination. Then, the received power for the EUT transmitting in the loaded RC $P_{r|l}$ was measured as described in Fig. 2d. Applying Equation (6) with G_l and $P_{r|l}$ gives $P_{Tx|l}$. As such, $P_{Tx|l}$ provided the net EUT TRP including absorption due to direct illumination on the phantom. The absorbed power $P_{Abs|Dir}$ excluding the effect of the chamber multipath reflections is therefore calculated as follows:

$$P_{Abs|Dir} = P_{Tx|u} - P_{Tx|l} \tag{7}$$

WBSAR was then obtained by using Equation (3). The body mass m_{WB} was conservatively chosen as the whole-body child mass of 12.5 kg specified in IEC 62232 [11]. The steps in Fig. 2(a) and (c) to characterize the chamber transfer functions

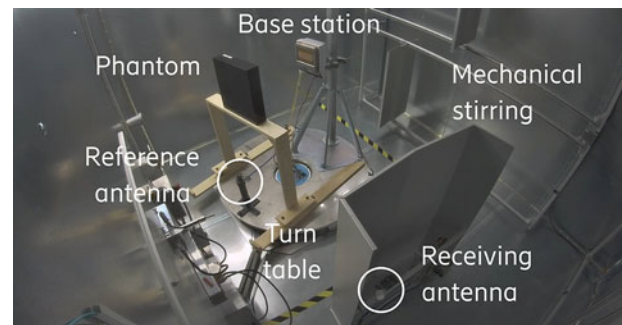


Figure 3. Measurement setup inside of the RC.

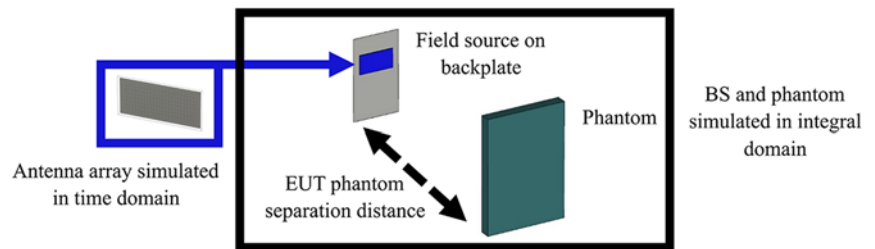
G_u and G_l were conducted once for a specific EUT. The measurements of $P_{Tx|u}$ (Fig. 2(b)) depend on the EUT configurations (in terms of the selected frequency band, channel, or operating beam) and were repeated for each EUT configuration. $P_{Abs|Dir}$ is additionally dependent on the distance and orientation of the EUT with respect to the phantom. Hence, for each EUT-phantom distance, the step described in Fig. 2(d) was repeated.

Equipment

The measurement setup inside the Bluetest RTS85HP RC is shown in Fig. 3. The dimension of Bluetest RTS85HP is 2260 mm × 2360 mm × 2480 mm. The RC can operate from 450 MHz to 67 GHz. A list of equipment is presented in Table A1.

Table 1. Horn antenna and AIR 1281 max gain, TRP, horizontal and vertical HPBW

Antenna		Max gain [dBi]	TRP [mW]	Horizontal HPBW [°]	Vertical HPBW [°]
Horn		14.9	160	35.8	31.9
AIR 1281	Boresight	29.0	440	4.1	10.4
	Steered	25.5	330	8.0	10.0

**Figure 4.** Illustration of the simulation of AIR 1281 and phantom.

Mechanical stirring, source moving stirring, and frequency stirring were used for the chamber transfer function measurements; mechanical stirring together with source moving stirring were used for the TRP measurement. Two EUTs including an A-INFO horn antenna and an Ericsson AIR 1281 B257 mmWave BS were measured in the RC. The maximum gain, measured TRP, and half power beam width (HPBW) of the EUTs are presented in Table 1. A signal generator and a power amplifier were used to feed the horn antenna. The AIR 1281 has beam steering and was set to operate constantly at the maximum rated TRP with a fixed beam for each measurement. Two beams were selected for the measurements, the boresight beam and a steered beam. The steered beam was steered -60° vertically and -15° horizontally from boresight. Both EUTs were set up to transmit a 5G test signal (3GPP conformance test model TM 3.1 [12]) at a center frequency of 28 GHz with a bandwidth of 100 MHz.

Currently, no phantom for evaluating WBSAR above 6 GHz has been standardized. The SPEAG mmW-BLAP-V1 rectangular-shaped phantom (375 mm \times 325 mm \times 75 mm) was used in this study. The phantom's bulk material has a relative permittivity of 18.6 and conductivity of 6.24 S/m at 28 GHz [13]. The phantom also has a coating with a maximum thickness of 0.2 mm, permittivity of 3.5, and conductivity of 1 S/m. This cuboid-shaped phantom was not explicitly designed for the purpose of characterizing WBSAR at mmWave frequencies, but its dielectric parameters are of relevance for the investigated band. A wooden cart was used to position the phantom in front of the transmitting antenna as can be seen in Fig. 3. G_I and G_u consider the losses in the wooden cart. In this study, the separation distance from the EUT to the phantom was varied from 1 to 70 cm.

Simulation

The WBSAR simulations with the phantom and EUTs were performed in CST Studio Suite 2022, using the integral solver based on the multilevel fast multipole method. Simplified models of the horn and the AIR 1281 were used. The horn antenna was made from perfect electric conductor (PEC) and a waveguide port. The AIR 1281 antenna array was simulated using the time-domain solver, to produce an equivalent field source, which was imported into the integral solver, as can be seen in Fig. 4. The main body of the AIR 1281 was approximated by

a PEC backplate placed on the back of the field source, which was used to model the reflections between the BS and the phantom.

The difference of the maximum gain and HPBW of the simplified antenna models was within 2% of the values in Table 1. The phantom was modeled as a PEC with coating that has the same surface properties as the mmW-BLAP-V1 phantom. The thickness of the coating was five times that of the skin depth to ensure all transmission into the phantom is absorbed, and the integral solver computes the total absorbed power inside the phantom by summing up the surface impedance loss while not computing the field inside the phantom to greatly reduce computational resource demands. The maximum cell size in the integral solver was 7 cells per wavelength for the horn and 10 cells per wavelength for the AIR 1281. In order to compare numerical and experimental data, the transmitted power in the simulation was set equal to the antenna TRP as measured in the chamber.

Results

The WBSAR simulations and measurement results for the AIR 1281 and horn antenna are presented in Fig. 5. The WBSAR measurements were performed at nine separation distances between the EUT and phantom from 1 to 70 cm. Simulations and measurements are in very good agreement with an average difference in WBSAR of 2% for the AIR 1281 boresight beam and 11% for the horn antenna. The corresponding maximum difference is 4% and 13% for the AIR 1281 and the horn antenna, respectively. The average and maximum difference for the steered beam of the AIR 1281, for separation distances from 1 to 10 cm is 18% and 34%, respectively. The difference between measurements and simulations is due to the measurement uncertainty as well as to the approximation in the numerical models. WBSAR decreases with the increasing EUT-phantom separation distance, since the phantom becomes smaller compared to the beam size at increasing separation distances. For distances larger than 10 cm, almost no energy from the steered beam of AIR 1281 intercepts the phantom, and WBSAR for this configuration is almost zero (due to the uncertainty, when $P_{Tx|I}$ approaches $P_{Tx|u}$, the calculated $P_{Abs|Dir}$ can be negative; in this case, the measured WBSAR was set to zero).

The smallest EUT-phantom separation distance of 1 cm gave the largest WBSAR at 0.035 W/kg for AIR 1281 boresight beam (with TRP of 440 mW), 0.025 W/kg for AIR 1281 steered beam (with TRP of 330 mW) and 0.009 W/kg for the horn antenna (with TRP

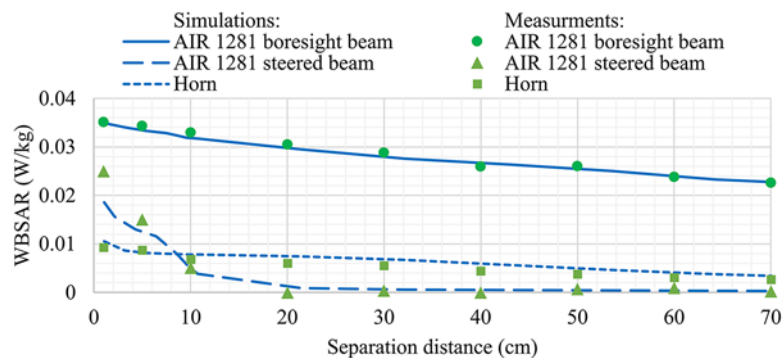


Figure 5. WBSAR measurement and simulation results for the AIR 1281 mmWave massive MIMO BS and the horn antenna.

of 160 mW). All the measurements are well below the 0.08 W/kg WBSAR limit specified in ICNIRP 2020 and applicable for the general public.

Discussion

The results show good agreement between measurements and simulations. The method provides an innovative and efficient way to measure WBSAR at mmWave frequencies, in accordance with the ICNIRP 2020 guidelines. When G_u and G_l are established, a WBSAR measurement can be done in 3 minutes (with the measurements of $P_{Tx|u}$ and $P_{Tx|l}$ taking 1.5 minutes each). The measurements of the chamber transfer functions are performed only once with G_u and G_l taking 15 minutes each.

Future studies will be needed to characterize the uncertainty of the measurement method. For instance, a limitation with the proposed methodology is that the phantom, when in proximity of the EUT, could induce an antenna mismatch which cannot be experimentally evaluated if the antenna ports are not accessible. With the given methodology, the power which is reflected at the antenna port is assumed absorbed by the phantom, possibly leading to an overestimate of WBSAR, when measured at small EUT-phantom separation distances. The frequency range of the method should also be investigated since RCs can operate at frequencies lower and higher than 28 GHz; the method could potentially help with reducing the measurement time at the lower frequencies compared with conventional methods applicable below 6 GHz.

For transmitters operating below 1 W (or more, if the BS is installed at a minimum height of 2.2 m) compliance with the whole-body exposure limits can generally be shown by means of exclusion criteria [11] without requiring any further assessment. For higher power levels, WBSAR measurements in RC provides a solution for assessing product compliance of BSs directly with the ICNIRP basic restrictions and for separation distances of 1–2 m depending on the size of the RC.

Conclusions

An efficient method to measure WBSAR from mmWave BSs has been presented in this paper. The method is based on measuring the TRP of the EUT and the TRP from the EUT and phantom combined, whose difference results in the phantom total absorbed power. The contribution from absorption due to the EUT direct illumination of the phantom is distinguished from that caused by the multipath reflections in the RC, making this technique suitable for EMF product compliance assessment with ICNIRP 2020 whole-body basic restrictions of BSs for short separation distances

(as limited by the dimension of the RC). Comparing simulations to measurements demonstrates good agreement at 28 GHz. For the beam configuration leading to maximum exposure, the difference between simulations and measurements for the Ericsson AIR 1281 massive multi-input–multi-output BS was on average 2% and at maximum 4%. For the horn antenna the average difference was below 13%. Furthermore, the measurements are fast, with each measurement taking 3 minutes once the chamber transfer functions have been established.

Competing interests. The author(s) declare none.

References

- Hill DA (2009) *Electromagnetic Fields in Cavities: Deterministic and Statistical Theories*, IEEE Press Series on Electromagnetic Wave Theory, vol. 35. New York: John Wiley & Sons.
- Andrie G (2021) *Electromagnetic Reverberation Chambers Recent Advances and Innovative Applications*. London: The Institution of Engineering and Technology.
- Furth B and Ahson S (2009) *Long Term Evolution: 3GPP LTE Radio and Cellular Technology*. New York: Taylor & Francis.
- Wang J, Suzuki T, Fujiwara O and Hariama K (2012) Measurement and validation of GHz-band whole-body average SAR in a human volunteer using reverberation chamber. *Physics in Medicine & Biology* 57(23), 7893.
- Kvarnstrand J, Schilliger Kildal S, Skårbratt A and Schilliger Kildal M (2016) Comparison of live person test to head and hand phantom test in reverberation chamber. In *10th European Conference on Antennas and Propagation (EuCAP)*, Davos Switzerland.
- Gifuni A, Adil M, Grassini G, Buono A, Nunziata F, Micheli D and Migliaccio M (2022) An effective method using reverberation chambers to measure TRP from mobile phones and power absorbed by user body. In *IEEE Transaction on Electromagnetic Compatibility*.
- Eilers Bischoff J (2022) Whole-body SAR measurements of 5G mmW base stations in a reverberation chamber. KTH Royal Institute of Technology (Master Thesis), Sweden.
- International Commission on Non-Ionizing Radiation Protection (ICNIRP) (2020) Guidelines for limiting exposure to electromagnetic fields (100 kHz to 300 GHz). *Health Physics* 118(5), 483–524.
- ICNIRP (1998) Guidelines for limiting exposure to time-varying electric, magnetic and electromagnetic fields (up to 300 GHz). *Health Physics* 74(4), 494–522.
- Colombi D, Xu B, Anguiano Sanjurjo D, Joshi P, Ghasemifard F, Di Paola C and Törnevik C (2022) Implications of ICNIRP 2020 exposure guidelines on the RF EMF compliance boundary of base stations. *Frontiers in Communications and Networks* 3, 744528.
- International Electrotechnical Commission (2022) Determination of RF field strength, power density and SAR in the vicinity of radiocommunications base stations for the purpose of evaluating human exposure. Standard IEC 62232 ED3.

12. **3GPP** (2023) 5G; NR; Base Station (BS) conformance testing Part 2: Radiated conformance testing ETSI TS 138 141-2 V17.9.0 (2023-05).
13. **SPEAG LOSSY MATERIALS**, Schmid & Partner Engineering AG. <https://speag.swiss/components/dielectric-database/material-properties/> (accessed 16 October 2023).

Appendix

Table A1. List of equipment

Type	Manufacturer	Model
Phantom	SPEAG	mmW-BLAP-V1
RC	Bluetest AB	RTS85HP
Reference antenna	Bluetest AB	6–67 GHz
Receiving antenna	Bluetest AB	6–67 GHz
Signal analyzer	Rohde and Schwarz GmbH	FSVA40
VNA	Rohde and Schwarz GmbH	ZNA
Horn antenna	A-info Inc.	LB-SJ-180400
BS	Ericsson	AIR 1281 B257
Signal generator	Rohde and Schwarz GmbH	SMBV100B, SGS100A, SGU100A
Power amplifier	Exodus Advanced Communications	MPA2005



Jens Eilers Bischoff received the B.S. and M.S. degrees in electrical engineering from KTH Royal Institute of Technology in 2022. He is currently working with Ericsson Research, Stockholm, Sweden, with research related to radio frequency exposure from wireless communication equipment, specifically 5G.



Paramananda Joshi received the B.E. degree in electronics and communication from Tribhuvan University, Kathmandu, Nepal, in 2008, and the M.Sc. degree in wireless communication from Lund University, Lund, Sweden, in 2012. Since 2012, he has been with Ericsson Research, Stockholm, Sweden, where he is currently working as a Senior Researcher and also involved in research activities related to realistic radio frequency (RF) electromagnetic fields (EMF)

exposure from radio base stations and user devices. Since 2016, he has been working as the Technical Manager of the Ericsson EMF Research Laboratory, Stockholm.



Davide Colombi received the M.Sc. degree (summa cum laude) in telecommunication engineering from the Politecnico di Milano, Milan, Italy, in 2009. Since 2009, he has been with Ericsson Research, Stockholm, Sweden, where he is currently working with research related to radio frequency exposure from wireless communication equipment, particularly for 5G. Mr. Colombi was a recipient of the 2018 IEC 1906 Award. He has contributed to the development of IEC, ITU, and the IEEE standards on the assessment of radio frequency exposure from wireless equipment as an Expert, an Editor, and a Convener.



Bo Xu received the B.E. degree in information engineering from Zhejiang University, Hangzhou, China, in 2010, and the Ph.D. degrees (joint doctoral program) in optical engineering and electrical engineering from Zhejiang University, Hangzhou, China, and from the KTH Royal Institute of Technology, Stockholm, Sweden, in 2017 and 2021, respectively. He has been with Ericsson Research, Ericsson AB, Stockholm, Sweden, since 2018, and currently is a Senior Specialist in EMF Compliance Solutions. His research interests include electromagnetic field health and safety, mobile communication technologies, and antenna measurements. Dr. Xu has been an expert in the IEC Technical Committee 106 Joint Maintenance Team 62209-3 since May 2021.



Christer Törnevik (Member, IEEE) received the M.Sc. degree in applied physics from the Linköping University, Linköping, Sweden, in 1986, and the Licentiate degree in materials science from the Royal Institute of Technology, Stockholm, Sweden, in 1991. He joined Ericsson in 1991. Since 1993, he has been involved in research activities related to radio frequency exposure from wireless communication equipment. He is currently a Senior Expert with responsibility for electromagnetic fields and health within the Ericsson Group. From 2003 to 2005, he was the Chairman of the Mobile and Wireless Forum, where he is currently the Secretary of the Board. Since 2006, he has been leading the Technical Committee on electromagnetic fields of the Swedish Electrotechnical Standardization Organization, SEK, and he has as an expert contributed to the development of several CENELEC, IEC, ITU, and IEEE standards on the assessment of RF exposure from wireless equipment.